Mitigation of Unwanted Forward Narrow-band Radiation from PCBs with a Metamaterial Unit Cell

Ruaro, Andrea; Thaysen, Jesper; Jakobsen, Kaj Bjarne

Published in:
Proceedings of European Microwave Conference 2013

Publication date:
2013

Mitigation of Unwanted Forward Narrow-band Radiation from PCBs with a Metamaterial Unit Cell

Andrea Ruaro*†, Jesper Thaysen*, and Kaj B. Jakobsen†

*GN ReSound A/S, Lautrupbjerg 7, DK-2750 Ballerup, Denmark
†Department of Electrical Engineering, Technical University of Denmark, DK-2800 Lyngby, Denmark

***Abstract*—Mitigation of EMI from a PCB is obtained through the use of a metamaterial unit cell. The focus is on the reduction of narrow-band radiation in the forward hemisphere when the resonant element is etched on a layer located between the source of radiation and the ground plane. As opposed to previous publications in the literature, the aim of this work is the application of a filter to scattered radiation, generalizing the former characterizations based solely upon transmission lines' insertion loss. The radiating area accounts for traces and components placed on the top layer of a PCB and is simulated via a patch antenna. The study exhibits how the radiation pattern and the electric field on the patch antenna change within and outside the resonance bandwidth of the parasitic element. An EMC assessment provides experimental verification of the operating principle.**

***Index Terms*—Metamaterial filters; planar filters; electromagnetic interference (EMI); electromagnetic compatibility (EMC); printed circuit boards (PCB)**

I. Introduction

The traces on a printed circuit board (PCB) can act as radiation sources, and thus be at the origin of electromagnetic interference (EMI) problems. The primary consequence of this is products that interferes with nearby devices and ultimately that cannot be commercialized. In high-density, complex environments where radio and digital subsystems coexist, high-speed traces necessarily cross the RF circuitry. Most of these devices are severely space-constrained — e.g., hearing aids, mobile phones and handsets, medical implants, and the like.

In this context there is an interest in further suppressing the narrow-band EMI generated by RFICs, like power amplifier (PA) harmonics or local oscillator (LO) leakage [1], [2], in order to fulfil the EMC regulations. In particular, when the unwanted frequency is close to that which a system is intended to operate at, traditional techniques (e.g., decoupling capacitors) are not an effective solution if the desired signal has to be safeguarded. When the radiation source is placed on the top layer, or is anyway not shielded by, e.g., a power plane, the action traditionally takes place on the radiation path placing extra shields. Additional shields are costly, of complex implementation production-wise, and in particular can seriously compromise the functioning of small antennas nearby, as in the case of hearing aids.

Among filter techniques, electromagnetic bandgap (EBG) structures [3]–[6] cannot be used in space-constrained devices due to their dimensions, not even in a planar implementation. The use of mu-negative (MNG) resonators as filters for transmission lines was explored in the past [7], but coupling to microstrip lines demands complementary designs, e.g., complementary split-ring resonators, due to the direction of the fields necessary to excite the resonators [8]. Nevertheless, this kind of complementary designs [9] or in general defected ground structures (DGS) affects the currents running on the PCB, degrading the signal integrity performance and potentially creating EMC problems. A further performance worsening is even possible when the PCB is connected to a $\lambda/4-$monopole antenna that ideally requires a solid ground plane. The epsilon-negative (ENG) structure used here was introduced in [10] and it has been used in the literature mostly to enhance the radiation characteristics of electrically-small antennas [11], [12].

Therefore the issue is to reduce the radiation in the forward hemisphere without acting directly on the radiation path. For this purpose, this work makes use of a metamaterial-inspired near-field resonant parasitic (NFRP) element etched in an inner layer. The implementation allows to mitigate narrow-band EMI in electrically- and physically-small devices, where the rejection frequency is close to the signal frequency, the actual radiation source is unknown within a certain area, and where to preserve a solid ground is necessary to satisfy the antenna needs. A drawback of the implementation is the dedicated use of a part of an inner layer, which results in an increased PCB design complexity.

The article is organized as follows. Section II defines the problem geometry and describes the physical mechanism that the device is grounded on. Section III provides the full design data, as well as the simulation results and discussion. Section IV characterizes the effects of the structure on the EMC performance. Finally, Section V summarizes the findings.

II. Geometry and Theory

The stack-up, shown in Fig. 1, is on three layers: on the top layer there is a radiation source, namely a number of PCB traces randomly oriented within a certain area; on the inner

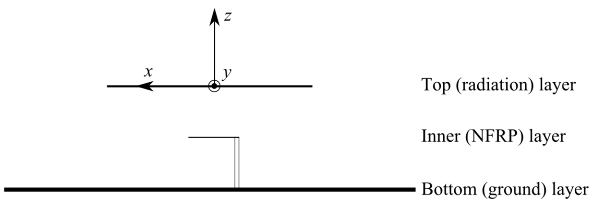

Fig. 1: PCB side view showing the radiation layer, the layer where the filtering structure can be implemented, and the ground plane.

layer there is a near-field resonant parasitic (NFRP) element connected to ground through a via; the third layer is a solid ground plane.

The forward hemisphere is defined with the coordinate system centred at the radiation source plane with the z axis oriented normal to the surface.

A patch antenna model is used to account for the PCB lines acting as radiation sources. This choice allows currents to run freely (and then be visualized) on a 2-D conductive surface, i.e., beyond the boundaries of a single line.

The NFRP element consists of a closely meandered line acting as an ENG metamaterial unit cell. It is chosen here for its marked sub-wavelength dimensions. It has been preferred over a MNG metamaterial unit cells due to its effective coupling mechanism to the target sources under examination, and to exploit the potential of directional filtering [13].

As known from the cavity model [14], the main radiation sources in a patch antenna are two equivalent magnetic dipoles along the patch width, with the electric field oriented normal to the ground plane. The NFRP structure is excited by such a field and drives the radiation to ground through the via connection. The resonator is thus placed in close proximity to one of the radiating slots in order to maximize the coupling. Even though most of the radiation comes from these equivalent sources, they are not the only parts of the patch actually radiating: the antenna is thus considered representative of scattered radiation, where the two radiating slots have dominant behaviour. This can easily recall the scenario of a PCB, with a microstrip line radiating as the major contributor and any other, differently oriented, acting as secondary contributors.

The structure fulfils the implementation requirements, namely to be physically- and electrically-small, to leave substantially unaltered the ground plane, and to have a narrow-frequency transition band.

III. Simulation Set-up and Results

A. Set-up

The geometry is shown in Fig. 2. The circuit is simulated with Ansys HFSS [15] and fabricated on a FR-4 substrate with a dielectric constant $\varepsilon_r = 4.4$. The height of the inner layer over the ground layer is $h_{\text{in}} = 0.8$ mm, while the height of the top layer with respect to the same reference is $h_{\text{top}} = 1.6$ mm. The ground plane dimensions are 150 mm $\times$ 150 mm.

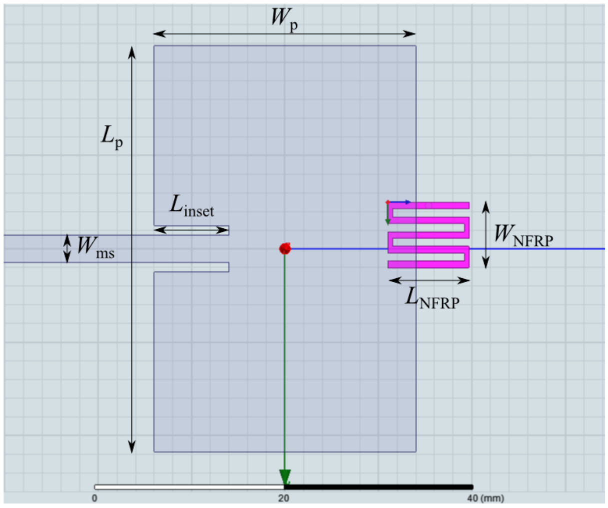

Fig. 2: Top view, with geometry outlined.

TABLE I: Patch antennas dimensions (in mm)

	2.45 GHz	2.85 GHz
W	43.5	37.4
L	28.0	24.2
W_{ms}	3.0	3.0
L_{inset}	8.0	7.0

The metallization is made of copper with thickness $t = 35$ μm.

Two patch antennas are designed to account for two signals with different frequencies. The desired signal frequency is chosen at 2.45 GHz, so that it falls within the ISM band, while the rejection frequency is chosen to be 2.85 GHz. The latter is the frequency at which the NFRP element is resonant. The patch antenna dimensions can be found in Table I. The feed is via a recessed microstrip transmission line.

The NFRP element counts 5 strips and 4 gaps. Its overall dimensions are $L_{\text{NFRP}} = 8.67$ mm $\times$ $W_{\text{NFRP}} = 7.04$ mm, with a microstrip width of $W_{\text{NFRP,ms}} = 0.72$ mm and a gap width of $W_{\text{NFRP,gap}} = 0.86$ mm.

B. Results

The goal of the results presented in this section is twofold: first, to show that the NFRP structure effectively suppress the interference emitted by a radiation source in the forward hemisphere; and second, to examine the effect that the same structure has on a frequency close to the one that has to be cancelled.

The two patch antennas have similar radiation characteristics. Table II shows their maximum directivity D_0 and their radiation efficiency e_{rad}. This similarity between the two structures can as well be noticed by comparing the electric field distributions in Fig. 3a and Fig. 4a and the radiation patterns (solid line in Fig. 5a and Fig. 5b).

When the NFRP structure is inserted in the inner layer, it can be seen in Fig. 3b that the distribution of the electric field

TABLE II: Directivity and radiation efficiency

		2.45 GHz	2.85 GHz
w/o NFRP	D_0	5.71	4.89
	e_{rad}	0.42	0.45
w/ NFRP	D_0	5.53	4.91
	e_{rad}	0.42	0.09

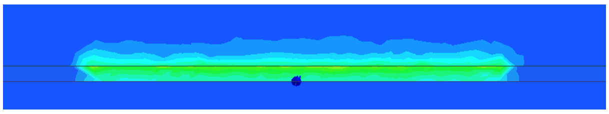

(a)

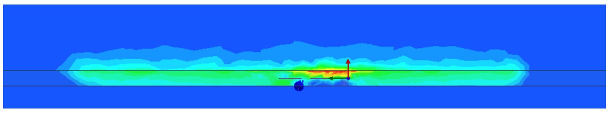

(b)

Fig. 3: Simulated electric field in the xz plane at the patch edge at 2.45 GHz, without (a) and with (b) the NFRP structure, respectively.

at 2.45 GHz is locally modified, getting stronger nearby the element. This is mostly due to the fact that the same field strength is confined in a smaller volume, since the NFRP has the same potential as the ground (especially close to the via connection). This does not influence the radiation pattern in a significant way, as read in Fig. 5a, nor the radiation efficiency reported in Table II.

On the contrary, when the element is inserted below a source at the frequency that is intended to cancel, it reduces the electric field strength along the radiation slot as can be seen in Fig. 4b. This does not affect the overall directivity in itself but rather the radiation efficiency of the patch, which is noticeably reduced by a factor of 5, and thus ultimately the radiation pattern as shown by the dotted line in Fig. 5b.

This shows the effectiveness of the NFRP in reducing the forward gain, and that the element is practically invisible outside the band that it is intended to reject.

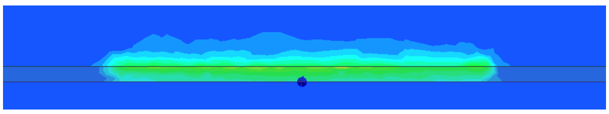

(a)

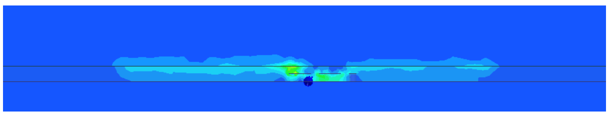

(b)

Fig. 4: Simulated electric field in the xz plane at the patch edge at 2.85 GHz, without (a) and with (b) the NFRP structure, respectively.

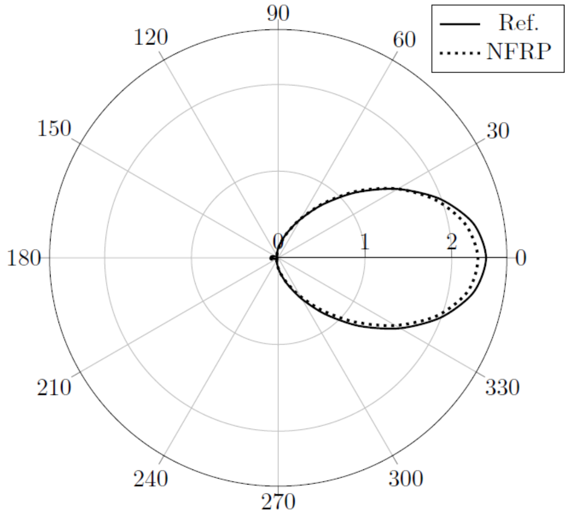

(a)

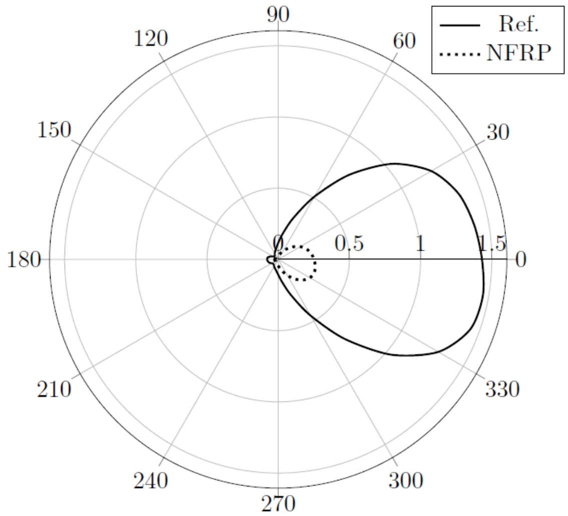

(b)

Fig. 5: Simulated gain pattern in the xz plane for the 2.45 GHz (a) and the 2.85 GHz (b) patch antenna with (dotted line) and without (solid line) the NFRP structure beneath.

IV. EMC Performance

A study of the effectiveness of the structure to reduce the EMI from the board has been performed as experimental verification. The source of EMI radiation, namely any signal trace on PCBs, is again modelled via a patch antenna. This permits to have a significant radiation at the frequency of interest, allowing for better measurements. It has the drawback of acting as an actual antenna, and thus to be loaded by the presence of the resonator. The patch is tuned to the resonance frequency of the ENG element. The measured values are afterwards normalized with respect to the frequency of interest for the sake of comparison with the results from the previous section. A reference board, comprising of the same radiation

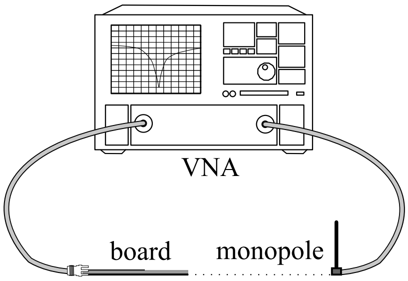

Fig. 6: Measurement setup for the study of radiation leakages in the xy (edge) plane.

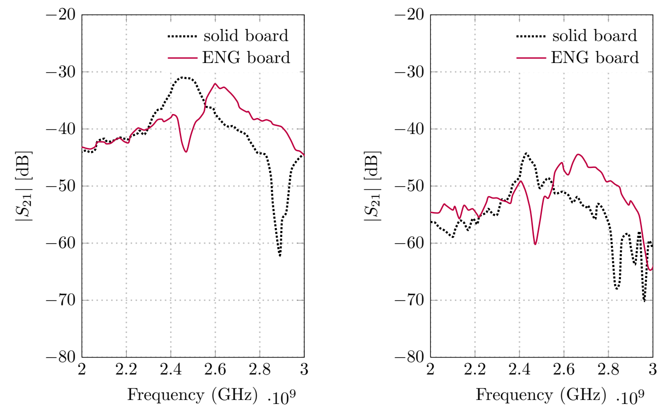

(a) (b)

Fig. 7: Leakage radiation in the xy (edge) plane, with the probe placed 5 cm (a) and 40 cm (b) away from the edge of the PCB, respectively.

source but without the ENG resonator, is used for comparison purposes. That being so, the results should be understood in a qualitative way.

The radiated fields are measured by the use of a monopole antenna at different positions and distances from the board in the xy (board edge) plane. The results in Fig. 7a and Fig. 7b are sampled at the edge plane with the setup shown in Fig. 6, progressively increasing the distance from the board. The valley caused by the resonator, that reduces the unwanted frequency of approximately 6 to 8 dB, is clearly visible. This is due to fact that the fields diffracted from the source edge are strongly coupled to the ENG structure and then dissipated in the ground plane. It is of interest to notice that they are not re-radiated along the edge plane, as has been observed in the literature for some EBG designs [6], [9]: thus the system is effectively reducing the radiation at the target frequency.

Due to the specific setup used here, i.e., a patch antenna as a radiation source, a noticeable shift in the frequency of the radiation peak is observed. This is most likely due to the loading effect of the ENG resonator on the patch, that changes its effective electrical length and the way that the device radiates—the actual attenuation has been corrected for this dependency of the setup. Please note, this frequency shift would not be compatible with the case of a radiating line.

V. Conclusion

In this work it was shown that it is possible to reduce the narrow-band EMI of a radiating source, in this case modelled via a patch antenna, through the use of a metamaterial-inspired near-field resonant parasitic element. The result is achieved with an extremely small structure that leaves substantially unaltered the ground plane characteristics. This accounts for an actual filtering not only as referred to the insertion loss of a line, but for the part radiated by a line and thus it qualifies as a way to reduce the interference radiated by transmission lines on boards.

References

[1] A. Abidi, "Direct-conversion radio transceivers for digital communications," *IEEE Journal of Solid-State Circuits*, vol. 30, no. 12, pp. 1399–1410, 1995.
[2] B. Razavi, "Design considerations for direct-conversion receivers," *IEEE Transactions on Circuits and Systems II: Analog and Digital Signal Processing*, vol. 44, no. 6, pp. 428–435, 1997.
[3] S. Shahparnia and O. Ramahi, "Electromagnetic interference (EMI) reduction from printed circuit boards (PCB) using electromagnetic bandgap structures," *IEEE Transactions on Electromagnetic Compatibility*, vol. 46, no. 4, pp. 580–587, 2004.
[4] M. Kim, K. Koo, C. Hwang, Y. Shim, J. Kim, and J. Kim, "A Compact and Wideband Electromagnetic Bandgap Structure Using a Defected Ground Structure for Power/Ground Noise Suppression in Multilayer Packages and PCBs," *IEEE Transactions on Electromagnetic Compatibility*, vol. 54, no. 3, pp. 689–695, Jun. 2012.
[5] F. D. Paulis and L. Raimondo, "Compact Configuration for Common Mode Filter Design based on Planar Electromagnetic Bandgap Structures," *IEEE Transactions on Electromagnetic Compatibility*, vol. 54, no. 3, pp. 646–654, 2012.
[6] J. Qin, O. Ramahi, and V. Granatstein, "Novel planar electromagnetic bandgap structures for mitigation of switching noise and EMI reduction in high-speed circuits," *IEEE Transactions on Electromagnetic Compatibility*, vol. 49, no. 3, pp. 661–669, 2007.
[7] J. Baena and J. Bonache, "Equivalent-circuit models for split-ring resonators and complementary split-ring resonators coupled to planar transmission lines," *IEEE Transactions on Microwave Theory and Techniques*, vol. 53, no. 4, pp. 1451–1461, 2005.
[8] R. Marqués, F. Medina, and R. Rafii-El-Idrissi, "Role of bianisotropy in negative permeability and left-handed metamaterials," *Physical Review B*, vol. 65, no. 14, p. 144440, Apr. 2002.
[9] M. M. Bait-Suwailam and O. M. Ramahi, "Ultrawideband Mitigation of Simultaneous Switching Noise and EMI Reduction in High-Speed PCBs Using Complementary Split-Ring Resonators," *IEEE Transactions on Electromagnetic Compatibility*, vol. 54, no. 2, pp. 389–396, Apr. 2012.
[10] P. D. Imhof, R. W. Ziolkowski, and J. R. Mosig, "Highly subwavelength unit cells to achieve epsilon negative (ENG) metamaterial properties," *IEEE Antennas and Propagation Society International Symposium 2006*, vol. 2, no. 1, pp. 1927–1930, 2006.
[11] A. Erentok and R. Ziolkowski, "Metamaterial-inspired efficient electrically small antennas," *IEEE Transactions on Antennas and Propagation*, 2008.
[12] C. Lin, P. Jin, and R. Ziolkowski, "Single, Dual and Tri-Band-Notched Ultrawideband (UWB) Antennas Using Capacitively Loaded Loop (CLL) Resonators," *IEEE Transactions on Antennas and Propagation*, vol. 60, no. 1, pp. 102–109, 2012.
[13] A. Ruaro, J. Thaysen, and K. B. Jakobsen, "Metamaterial-inspired Near-field Resonant Parasitic Structure for Directional Suppression of Narrow-band EMI/RFI in Compact Systems," in *2013 IEEE Antennas and Propagation Society International Symposium (APSURSI 2013)*, 2013.
[14] C. A. Balanis, *Antenna Theory: Analysis and Design*, 3rd ed. John Wiley & Sons, Inc., 2005.
[15] Ansys®, HFSS, Release 13.0.